Available online at www.sciencedirect.com
SCIENCE DIRECT®
Solid State Nuclear Magnetic Resonance 29 (2006) 163–169
Solid State Nuclear Magnetic Resonance
www.elsevier.com/locate/ssnmr

# A 1D sensitivity-enhanced $^{1}H$ spin diffusion experiment for determining membrane protein topology

Wenbin Luo, Mei Hong*

*Department of Chemistry, Iowa State University, Gilman 0108, Ames, IA 50011, USA*

Received 7 June 2005; received in revised form 10 August 2005
Available online 3 October 2005

**Abstract**

A sensitivity-enhanced 1D $^{1}H$ spin diffusion experiment, CHH, for determining membrane protein topology is introduced. By transferring the magnetization of the labeled protein $^{13}C$ to lipid and water protons for detection, the CHH experiment reduces the time of the original 2D $^{13}C$-detected experiment by two orders of magnitude. The sensitivity enhancement results from $^{1}H$ detection and the elimination of the $^{13}C$ dimension. Consideration of the spin statistics of the membrane sample indicates that the CHH sensitivity depends on the $^{13}C$ labeling level and the number of protein protons relative to the mobile protons. 5–35% of the theoretical sensitivity was achieved on two extensively $^{13}C$ labeled proteins. The experimental uncertainties arise from incomplete suppression of the equilibrium $^{1}H$ magnetization and the magnetization of lipid protons directly bonded to natural-abundance carbons. The technique, demonstrated on colicin Ia channel domain, confirms the presence of a transmembrane domain and the predominance of surface-bound helices.


*Keywords:* $^{1}H$ spin diffusion; Sensitivity enhancement; Lipid bilayer; Depth of insertion; Protein topology; Membrane proteins; Selective labeling

## 1. Introduction

$^{1}H$ spin diffusion between lipids and membrane-bound proteins was recently introduced as an approach for determining the depth of insertion of the protein in lipid bilayers [1]. Two experimental implementations have been demonstrated. In the original 1D experiment, the membrane sample is frozen to a temperature at which the lipids cease their fast uniaxial rotation while the inter-bilayer water remains partially mobile. This residual mobile water magnetization is then selected as the source of the $^{1}H$ magnetization and transferred to the rigid lipid and protein. Detection of the protein $^{13}C$ or $^{15}N$ signals as a function of the $^{1}H$ spin diffusion mixing time yields a buildup curve that can be simulated to yield the distance of the labeled site from the water at the membrane surface. Detection of the natural abundance $^{31}P$ or $^{13}C$ signals of the lipids with known distances from the membrane surface allows internal calibration of the $^{1}H$ spin diffusion coefficients [1,2].

In the second version of the $^{1}H$ spin diffusion experiment [3], the membrane sample is kept at ambient temperature where the lipids are in the liquid-crystalline state. The multiple mobile $^{1}H$ magnetization sources are resolved in the indirect dimension of a 2D spectrum by $^{1}H$ chemical shift evolution. Following $^{1}H$ evolution, the mobile $^{1}H$ magnetization is transferred to the rigid protein protons during a mixing time. The amount of the transferred magnetization, which depends on the proximity between the lipid moiety and the protein, is finally detected through the protein $^{13}C$ signals in the direct dimension. The $^{1}H$–$^{13}C$ cross peak intensities in the 2D spectra as a function of the spin diffusion mixing time give rise to the buildup curve, from which the shortest distance separation between the protein and the mobile proton source can be determined semi-quantitatively.

The key difference between the room-temperature 2D $^{1}H$ spin diffusion experiment and the low-temperature 1D experiment is that in the 2D experiment, the abundant motion of the fluid lipid bilayer makes its $^{1}H$ spin diffusion

*Corresponding author. Fax: +1 515 294 0105.
*E-mail address:* mhong@iastate.edu (M. Hong).

0926-2040/$ - see front matter © 2005 Elsevier Inc. All rights reserved.
doi:10.1016/j.ssnmr.2005.08.007

coefficient substantially smaller than that of the rigid protein, thus as soon as the lipid $^{1}H$ magnetization is transferred across the interface to the protein, the magnetization equilibrates rapidly in the rigid protein. As a result, the shape of the $^{1}H$ buildup curve is primarily determined by the shortest separation between the lipid source proton and the protein, and does not depend on the exact location of the specific $^{13}C$ or $^{15}N$ label in the protein. While less quantitative and lacking distance site resolution compared to the 1D experiment, the 2D experiment is well suited to extensively labeled proteins where single site resolution is not available to begin with. It can yield the global topology of the protein, such as the presence or absence of transmembrane domains, in large polytopic membrane proteins [3,4].

Despite its utility, the need for collecting a series of 2D spectra as a function of mixing time poses challenges in sensitivity and experimental stability. Since the intensities of several 2D spectra need to be compared, a long block of experimental time is necessary. Spinning hydrated membrane samples at ambient temperature for an extended period of time is prone to cause dehydration and thus changes in the $^{1}H$ $T_1$ relaxation times. In addition, fluctuation in the radio frequency powers can affect the 2D intensity from one spectrum to another. For these reasons, it is desirable to increase the sensitivity of the room-temperature 2D spin diffusion experiment.

Indeed, sensitivity enhancement should be possible if one considers the fact that the 2D experiment puts the high-resolution $^{1}H$ chemical shift spectrum in the indirect dimension while the low-sensitivity $^{13}C$ chemical shift spectrum in the direct dimension. This means that not only the detection sensitivity is low, but also a large number of $t_1$ slices is necessary to resolve the different $^{1}H$ signals of the mobile lipid and water. Thus, a switch of the two dimensions would clearly be advantageous. Moreover, since the room-temperature spin diffusion experiment inherently does not resolve the depths of different $^{13}C$ sites within the protein, the $^{13}C$ dimension can in fact be removed altogether. In this paper, we demonstrate this simplified 1D $^{1}H$-detected spin diffusion experiment. We designate this experiment CHH, to represent the magnetization pathway of protein $^{13}C \rightarrow$ protein $^{1}H \rightarrow$ lipid and water $^{1}H$. In analogy, the 2D spin diffusion experiment will be called HHC, representing the reverse magnetization pathway of lipid and water $^{1}H \rightarrow$ protein $^{1}H \rightarrow$ protein $^{13}C$.

## 2. Materials and methods

### 2.1. Sample preparation

Colicin Ia channel domain (MW: 25 kDa) was expressed as described before [5,6] and labeled using the TEASE protocol [7], where the labeled carbon precursor is supplemented with unlabeled ten amino acids from the citric acid cycle to suppress the labeling of these mostly polar amino acids. 1,6-colicin was expressed using [1,6-$^{13}C$] glucose as the main precursor, resulting in the following $^{13}C$-labeled sites: Ala C$\beta$, Leu C$\alpha$, C$\delta$1, C$\delta$2, Ser C$\beta$, Val C$\gamma$1, C$\gamma$2, His C$\delta$2, C′, Phe C$\beta$, C$\gamma$, C$\delta$1, C$\delta$2, Tyr C$\beta$, C$\delta$1, C$\delta$2, C$\zeta$, and Trp C$\beta$, C$\delta$2, C$\varepsilon$1, C$\varepsilon$2 [6,8]. pU-colicin was expressed using [U-$^{13}C$] glucose as the $^{13}C$-labeled precursor, resulting in uniform $^{13}C$ labeling of Ala, Leu, Ser, Val, Gly, His, Phe, Tyr and Trp. Both protein samples were uniformly $^{15}N$ labeled using $^{15}N$-$NH_4Cl$.

The labeled colicin Ia channel domain was reconstituted into large unilamellar vesicles of POPC/POPG (3:7 molar ratio) membranes at pH 4.8 as described previously [6]. The protein/lipid molar ratio is 1:100. The membrane pellet obtained after ultracentrifugation was lyophilized, packed into a 4 mm MAS rotor, and hydrated to 35% water by mass.

### 2.2. Solid-state NMR experiments

All NMR experiments were carried out on a Bruker DSX-400 spectrometer (Karlsruhe, Germany) operating at a resonance frequency of 400.49 MHz for $^{1}H$ and 100.71 MHz for $^{13}C$. A double-resonance MAS probe with a 4-mm spinning module was used. The $^{1}H$ radiofrequency (rf) field strengths for TPPM decoupling [9] were ~65 kHz. Typical $^{13}C$ and $^{1}H$ 90° pulse lengths were 5 and 4 μs. The recycle delay ranged from 1.8 to 3 s. Cross-polarization (CP) contact times were 200 μs for the first CP and 150 μs for the second CP in the 1D CHH experiment. All experiments were conducted at room temperature (293 K) at a spinning speed of 5 kHz. The 1D CHH spectra were collected with mixing times of 1 μs to 625 ms. The pU-colicin required 32 or 64 scans per mixing time, while the 1,6-colicin used 128 or 256 scans per mixing time. Peak intensities were plotted as a function of the mixing time and corrected for $^{1}H$ $T_1$ relaxation as measured from a separate $T_1$ inversion recovery experiment. 2D HHC spectra were acquired with 64 or 128 scans per $t_1$ slice, 176 $t_1$ slices, and a $^{1}H$ spectral width of 5 kHz. $^{1}H$ mixing times of 25, 100 and 225 ms, were used for the 2D experiments on pU-colicin. States detection was used to obtain pure-phase spectra [10].

## 3. Results and discussion

### 3.1. CHH pulse sequence

The pulse sequence for the sensitivity-enhanced 1D CHH experiment with $^{1}H$ detection is shown in Fig. 1a. After $^{1}H$–$^{13}C$ CP, a 90° $^{13}C$ pulse stores the $^{13}C$ magnetization along the $z$-axis while the $^{1}H$ magnetization of both protein and lipids is destroyed by a $T_2$ filter. The $^{1}H$ $T_2$ filter includes two delay periods, $\tau_1$ and $\tau_2$, separated by a 90° pulse. A $\tau_1$ value of 20–30 ms and $\tau_2$ of 5 ms were used. The purpose of the 90° pulse is to rotate the $^{1}H$ magnetization that has undergone $T_1$ relaxation back to the transverse plane, to be destroyed by the second delay $\tau_2$. At the end of the $^{1}H$ $T_2$ filter, mostly only $^{13}C$ magnetization of the labeled sites in the protein remains. This is returned to the transverse plane by a $^{13}C$ 90° pulse, then transferred to the

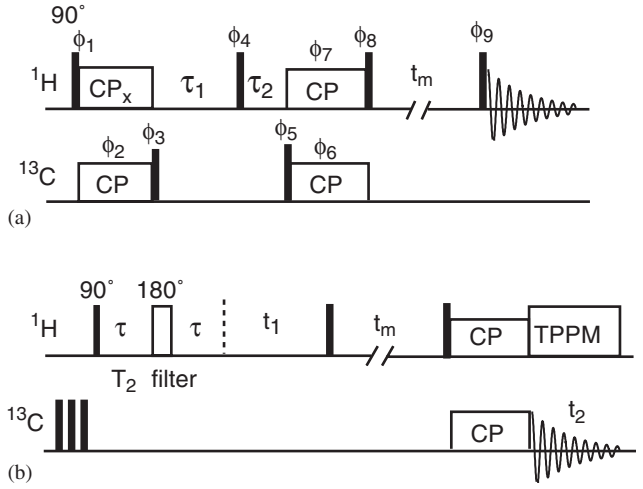


Fig. 1. Pulse sequences for (a) the 1D CHH experiment and (b) the 2D HHC experiment. In (a), $\tau_1 = 20-30$ ms and $\tau_2 = 5$ ms. CP times were 200 μs for the first CP and 150 μs for the second CP. In (b), $\tau = 1$ ms. Pulse sequence (a) used 32- or 64-step phase cycles. The 64-step phase cycles are: $\phi_1 = 1\ 3$; $\phi_2 = 0\ 0\ 1\ 1\ 2\ 2\ 3\ 3$; $\phi_3 = 1\ 1\ 2\ 2\ 3\ 3\ 0\ 0, 3\ 3\ 0\ 0\ 1\ 1\ 2\ 2$; $\phi_4 = 1\ 3$; $\phi_5 = 3\ 3\ 0\ 0\ 1\ 1\ 2\ 2$; $\phi_6 = (0\ 0\ 1\ 1\ 2\ 2\ 3\ 3) \times 2, (2\ 2\ 3\ 3\ 0\ 0\ 1\ 1) \times 2$; $\phi_7 = 0\ 0\ 1\ 1\ 2\ 2\ 3\ 3$; $\phi_8 = (1\ 1\ 2\ 2\ 3\ 3\ 0\ 0) \times 4, (3\ 3\ 0\ 0\ 1\ 1\ 2\ 2) \times 4$; $\phi_9 = 3\ 3\ 0\ 0\ 1\ 1\ 2\ 2$; $\phi_{10} = \bar{R}RR\bar{R}RR\bar{R}R$, where $R = 0\ 2\ 1\ 3\ 2\ 0\ 3\ 1$, and $\bar{R} = 2\ 0\ 3\ 1\ 0\ 2\ 1\ 3$. ($0 = x$, $1 = y$, $2 = -x$, $3 = -y$).

protein protons by a short $^{13}C$–$^{1}H$ CP step. The protein $^{1}H$ magnetization, flipped to the $z$-axis by a 90° pulse, then spin-diffuses to the mobile lipid and water, whose signals are detected without homonuclear decoupling. The intensity of the lipid and water $^{1}H$ signals transferred from the protein protons is monitored as a function of the spin diffusion mixing time. The resulting buildup curve is fit to give a semi-quantitative distance, which represents the shortest distance between the protein and the detected lipid or water protons.

For comparison, the pulse sequence for the 2D $^{13}C$-detected $^{1}H$ spin diffusion experiment [3] is shown in Fig. 1b. The key difference from the 1D experiment is that the site-resolved lipid and water $^{1}H$ chemical shift is encoded in the indirect dimension, while the result of spin diffusion is detected via the protein $^{13}C$ labels in the direct dimension. However, since this spin diffusion experiment, conducted at room temperature where there is significant mobility difference between the soft membrane and the rigid protein, does not give site-specific distances between individual protein $^{13}C$ sites and the lipid moiety [3], the $^{13}C$ resolution in the direct dimension is not useful. Thus, the 1D CHH experiment eliminates this $^{13}C$ dimension altogether and detects the $^{1}H$ spectrum instead. Due to the high mobility of the lipid and water protons in the membrane, it is possible to conduct straightforward $^{1}H$ detection, without multiple-pulse homonuclear decoupling. Thus the sensitivity enhancement over $^{13}C$ detection is simply proportional to $(\gamma_H/\gamma_C)^{3/2} = 8$. Combined with the reduction of the dimensionality, this results in an experimental time saving of two orders of magnitude, as we show below.

### 3.2. Sensitivity enhancement of the 1D CHH over the 2D HHC experiments

Fig. 2 compares the F1 projection of the 2D HHC spectra of pU-colicin with the $^{1}H$-detected 1D CHH spectra. The spectra of three mixing times: 25, 100, and 225 ms, are shown. The $^{1}H$ spectra were processed with an exponential line broadening of 10 Hz. It can be seen that the 2D HHC projections is noisier than the 1D CHH spectra due to the lower sensitivity of $^{13}C$ detection, and residual truncation wiggles for the water signal remain due to the limited evolution time of the $^{1}H$ dimension. The 2D spectra were acquired with 22528 scans for the 25 and 225 ms mixing time points (~13 h), and half that amount for the 100 ms time point. In comparison, the 1D spectra were acquired with 64 scans (~min), corresponding to a time saving of 180–350 fold.

Information on the populations of residues on the membrane surface versus the bilayer center can be obtained from the relative height of the water $^{1}H$ signal and the $CH_2$ signal. The fact that the water signal is much higher indicates that colicin Ia channel domain is predominantly located on the membrane surface. To verify that the 1D CHH experiment reproduces the $^{1}H$ spin diffusion behavior seen in the 2D experiment, Fig. 3(a) and (b) superimposes the complete buildup curves (open symbols) of pU-colicin from the 1D CHH spectra with the corresponding 2D data at three mixing times (filled symbols). The buildup intensities were corrected for $^{1}H$ $T_1$ relaxation and normalized by the equilibrium values at

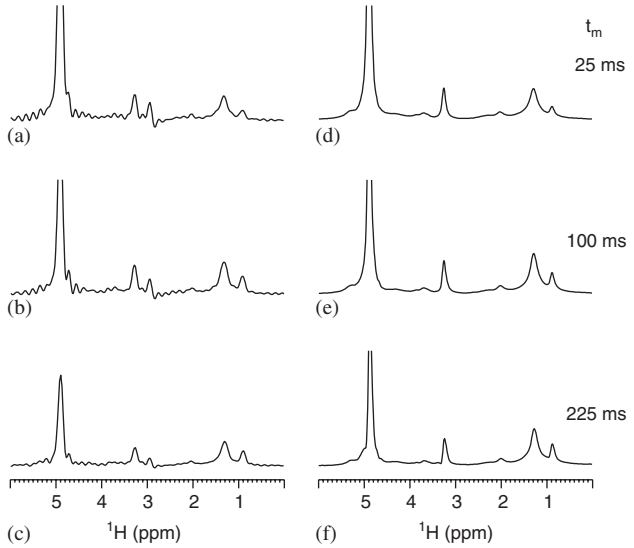


Fig. 2. Comparison of the $^{1}H$ spectra of pU-colicin from the 2D HHC experiment (a–c) and from the sensitivity-enhanced 1D CHH experiment (d–f) with the indicated mixing times. In each column, the spectra are drawn to scale after taking into account the number of scans. (a–c) F1 projection of the aliphatic region of the 2D HHC spectra. The peak at 3 ppm is a zero-frequency artifact. These 2D spectra were acquired with 11264 scans (b) and 22528 scans (a, c). (d–f) 1D CHH spectra, acquired with 64 scans. All spectra were processed with 10 Hz exponential line broadening.

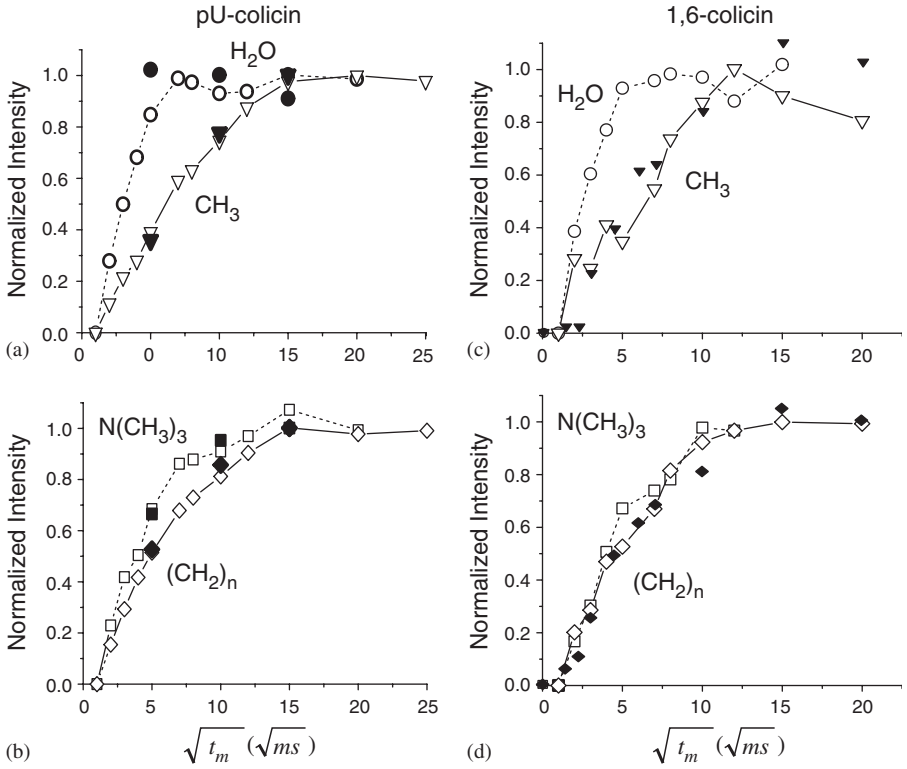


Fig. 3. Comparison between the $^{1}$H spin diffusion buildup curves from the 1D CHH experiment (open symbols) and from the 2D HHC experiment (filled symbols) at selected mixing times. (a, b) pU-colicin. (c, d) 1,6-colicin. The magnetization sources are $H_2O$ (circles), $N(CH_3)_3$ (squares), $(CH_2)_n$ (diamonds), and $CH_3$ (triangles). The 2D data in (c, d) are those of [2-13C] colicin Ia channel domain reproduced from Ref. [3]. For the pU-colicin data in (a, b), the error bar (including both random and systematic errors) is smaller than or comparable to the symbol sizes. For the 1,6-colicin data in (c, d), the random error is negligible but the systematic uncertainty is up to 30% for the $CH_2$ and $CH_3$ intensities, as indicated in Table 3.

long mixing times. It can be seen that the 1D buildup intensities superimpose well with the 2D data points, confirming that the same distance information is obtained. Specifically, the $CH_2$ and $CH_3$ buildup curves correspond to a short protein-lipid separation of ~2 Å, indicating that the protein contains a small but non-negligible fraction of residues that are transmembrane [3].

The 1D CHH buildup curves of the more sparsely $^{13}$C labeled 1,6-colicin reproduce the trend of the pU-colicin data as well as the buildup curves of [2-$^{13}$C] colicin reported previously [3] (Fig. 3c, d). However, the $CH_3$ buildup curve, obtained from the lowest intensity in the spectra, shows noticeable uncertainty. This results from the lower $^{13}$C labeling level, as we analyze below.

### 3.3. Sensitivity of the 1D CHH experiment

Since the 1D CHH experiment requires that all detected $^{1}$H magnetization originates from the labeled $^{13}$C sites in the protein, the sensitivity of the experiment depends critically on the $^{13}$C labeling level. The higher the $^{13}$C labeling level, the higher the CHH sensitivity. At the same time, the sensitivity of the experiment also depends on the fraction of the mobile protons in the entire proton reservoir, since only the $^{1}$H magnetization of the mobile lipid and water, not the rigid protein, is detected. The larger the fraction of the mobile protons, the more sensitive the CHH experiment.

The numbers of $^{1}$H spins in the protein ($H_P$), lipids ($H_L$) and water ($H_W$) for the two membrane-bound colicin Ia channel domain samples are tabulated in Table 1. These are estimated based on an experimental protein: lipid molar ratio of 1:100 and 35% (by mass) of water in the sample. The total number of the $^{1}$H spins in the system ($H_{tot}$) is the sum of the three. The number of labeled $^{13}$C spins in the protein ($C_P$) was calculated based on the labeling schemes used. $C_P$ of pU-colicin is about three times that of 1,6-colicin.

During the reverse CP step, the $^{13}$C magnetization is transferred to the protein protons. Assuming that the spin diffusion within the protein is rapid due to the rigidity of the molecule, we can estimate the fraction of the $^{13}$C magnetization that ends up in the proton reservoir during CP as $H_P/(H_P + C_P)$. This magnetization is then transferred to the mobile lipid and water molecules during the mixing time. Thus, at equilibrium, the effective number of detected protons in the CHH experiment is

$$H_{CHH} = C_P \times \frac{H_P}{H_P + C_P} \times \frac{H_L + H_W}{H_P + H_L + H_W}. \quad (1)$$

We define the ideal CHH sensitivity as the number of detected $^{1}$H spins, $H_{CHH}$, relative to the total number of

Table 1
Spin numbers and ideal CHH sensitivities for pU-colicin and 1,6-colicin

| | $H_P$ | $H_L$ | $H_W$ | $H_{tot}$ | $C_P$ | n.a. $^{13}C$[a] | $H_{CHH}$ | Sensitivity |
|---|---|---|---|---|---|---|---|---|
| pU-colicin | 1544 | 7780 | 6090 | 15414 | 513 | 50 | 346 | 2.5% |
| 1,6-colicin | 1544 | 7780 | 6090 | 15414 | 189 | 53 | 152 | 1.1% |

[a]The number of natural abundance lipid and protein $^{13}C$ spins in each sample.

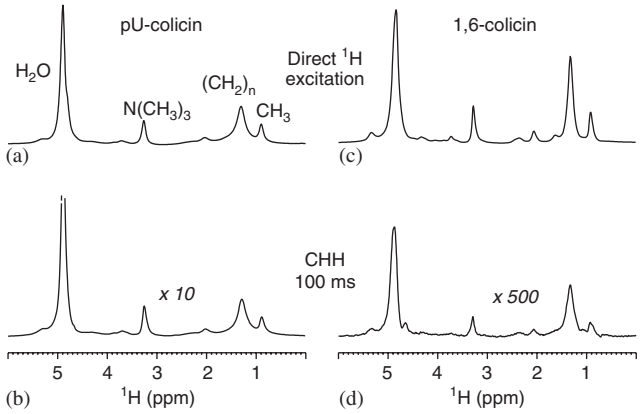


Fig. 4. Direct $^1H$ excitation spectra (a, c) and 1D CHH spectra (b, d) with a mixing time of 100 ms. (a, b) pU-colicin. (c, d) 1,6-colicin. Spectra (b, d) were scaled with respect to spectra (a, c) by the ratios shown. Numbers of scans (NS) are: (a) 4, (b) 64, (c) 32, and (d) 64. The intensities of the 100 ms CHH spectra relative to the direct excitation spectra after taking into account the NS difference are listed in Table 2.

Table 2
Experimental CHH sensitivities for pU-colicin and 1,6-colicin, obtained from the intensity ratio of the 100 ms CHH spectra with the $^1H$ direct excitation spectra

| | $H_2O$ | $N(CH_3)_3$ | $CH_2$ | $CH_3$ |
|---|---|---|---|---|
| pU-colicin | 0.90% | 0.85% | 0.63% | 0.64% |
| 1,6-colicin | 0.08% | 0.05% | 0.06% | 0.05% |

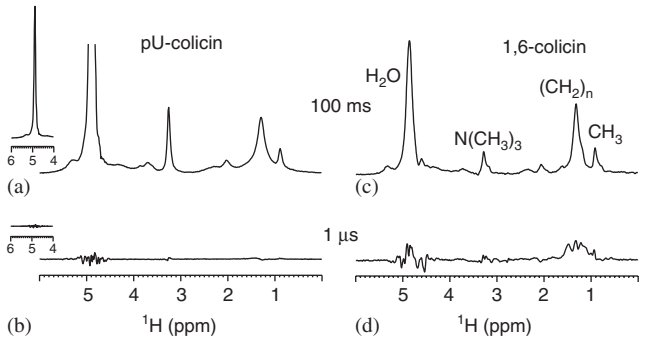


Fig. 5. CHH $^1H$ spectra of (a, b) pU-colicin and (c, d) 1,6-colicin, with spin diffusion mixing times of (a, c) 100 ms and (b, d) 1 µs. Insets of spectra (a, b) show the full heights of the water peak. The bottom spectra are plotted on the same scale as the top spectra in each column. NS are (a) 64, (b) 32, (c) 96, and (d) 96. The intensities of the 1 µs spectra relative to the 100 ms spectra after taking into account the NS difference are tabulated in Table 3.

lipid and water protons in the system:

$$\text{Sensitivity} = \frac{H_{CHH}}{H_L + H_W}. \quad (2)$$

Based on the $^{13}C$ labeling levels and the distribution of protons in the membrane samples, we find this ideal sensitivity to be 2.5% for pU-colicin and 1.1% for 1,6-colicin (Table 1), which represent the maximum sensitivity of the CHH spectrum relative to the equilibrium mobile $^1H$ magnetization.

Fig. 4 compares the $^1H$ direct excitation spectra with the 1D CHH spectra of pU-colicin and 1,6-colicin at a mixing time of 100 ms. The overall intensities of the 1D CHH spectra is two to three orders of magnitude lower than the direct excitation spectra. The experimental CHH sensitivities, obtained from the ratios of the individual CHH peaks (Fig. 4b, d) relative to the direct excitation peaks (Fig. 4a, c), are listed in Table 2. Although the CHH intensities are less than 1% of the direct excitation spectra, due to the high detection sensitivity of $^1H$, the random noise of the spectra is still negligible compared to the signal, at less than 1% of the signal. Indeed, the experimentally achieved CHH sensitivities are reasonable compared to the ideal sensitivity calculated for each sample. For pU-colicin, these are 25–35% of the ideal value, while for 1,6-colicin, the experimental CHH sensitivities is 5–10% of the ideal value.

### 3.4. Suppression of the direct lipid and water $^1H$ polarization

Since the 1D CHH experiment detects only a small fraction (<3% in our systems) of the total mobile proton magnetization, the clean suppression of the equilibrium lipid and water $^1H$ magnetization is crucial to the accuracy of the $^1H$ buildup curve. The suppression is mostly accomplished by the $^1H$ $T_2$ filter, during which $^1H$–$^1H$ dipolar coupling and transverse relaxation destroy the directly excited $^1H$ magnetization. The mechanism works well for the rigid protein protons; however, the suppression of the protons in the anisotropically mobile lipids and the isotropic water molecules is more difficult due to their motionally averaged dipolar couplings and long $T_2$ relaxation times. As an example, Fig. 5 shows the $^1H$ CHH spectra of the two membrane-bound colicin samples after a mixing time of 1 µs (b, d) and 100 ms (a, c). The former correspond to the no spin diffusion case, so any residual signals represent the unsuppressed and non-spin-diffused $^1H$ magnetization. In the more highly $^{13}C$-labeled pU-colicin, only the water peak is visible, while in the more sparsely labeled 1,6-colicin, the water and the $CH_2$ peaks both show noticeable residual intensities. The fractions of the residual $^1H$ intensities at 1 µs over the $^1H$ intensities at 100 ms are 3–5% for pU-colicin, but much higher values of 10–30% for 1,6-colicin (Table 3).

The residual equilibrium $^1H$ magnetization, when present, decreases the magnetization difference between the

source protons after the reverse CP and the sink protons, thus should cause a smaller slope in the $^1$H buildup curve. This in turn would result in an apparently longer protein-lipid distance. Indeed, this was found to be the case when incomplete suppression occurred in the absence of the 90° purge pulse in the $T_2$ filter period. This 90° pulse serves to rotate back to the transverse plane the $^1$H magnetization that has relaxed due to $T_1$ relaxation. The $^1$H $T_1$ values of the water and lipid protons in POPC/POPG membranes range from 250 to 450 ms. Thus, for a $\tau_1$ of 20 ms, 4–7% of the mobile proton magnetization would have relaxed to the $z$-axis. Although phase cycling removes most of this magnetization, it is still not negligible, considering that the percent of detected protons in the CHH experiment is only 1–3% (Table 1). By using this 90° purge pulse followed by another short dephasing period, we achieve more complete removal of the direct $^1$H magnetization. The effect of the 90° purge pulse and $\tau_2$ on the spin diffusion buildup curve is shown in Fig. 6. The addition of the purge pulse and $\tau_2$ resulted in faster buildup for all resolved proton species. The increased buildup rate is particularly pronounced for the $CH_2$ and $CH_3$ signals from the hydrophobic interior of the membrane, probably due to the fact that the majority of colicin Ia channel domain is bound immediately at the membrane surface that the initial rates for water and headgroup $\gamma$ protons are already high even in the absence of the purge pulse, while the buildup rates of the $CH_2$ and $CH_3$ are generally slower than the surface protons.

From this analysis, it can be seen that the main source of uncertainty of the 1D CHH experiment is the systematic error introduced by the incomplete suppression of the non-spin diffused $^1$H magnetization of lipid and water. For pU-colicin, which has a protein $^{13}$C labeling level of 53%, the signal-to-noise ratio of the water peak in the 25 ms CHH spectrum is ~1700 (Fig. 2d). This translates into a random noise of 0.06%. In comparison, the error from the unsuppressed initial $^1$H magnetization is 3% (Table 3), significantly higher than the random noise. Thus, better suppression techniques will be desirable for improving the applicability of this technique. The current 1D CHH experiment used extended phase cycles of 32 or 64 steps (Fig. 1). Potentially, gradient pulses may be used to achieve better suppression in fewer scans. Cleaner suppression of the initial $^1$H magnetization will make this 1D CHH technique more robust for proteins with lower labeling levels such as site-specifically labeled membrane peptides.

Table 3
CHH intensity ratios between spectra acquired with mixing times of 1 μs and 100 ms

| | $H_2O$ | $N(CH_3)_3$ | $CH_2$ | $CH_3$ |
|---|---|---|---|---|
| pU-colicin | 3% | 4% | 4% | 5% |
| 1,6-colicin | 10% | 20% | 30% | 30% |

The 1,6-colicin sample gives experimental CHH sensitivities that are lower than pU-colicin by more than the $^{13}$C labeling level difference. We attribute this to the fact that 1,6-colicin is predominantly labeled in the mobile side-chains, thus have less efficient CP transfer from $^{13}$C to $^1$H. 1,6-colicin also shows much larger residual $^1$H magnetization than pU-colicin in the limit of no spin diffusion mixing (Table 3). This partly results from the increased fraction of natural abundance lipid $^{13}$C sites (Table 1), which, during the reverse CP step, can give rise to $^1$H intensities that do not originate from the protein. Indeed, a control experiment using a membrane sample without the protein showed non-negligible $CH_2$ peak intensities at short mixing times (data not shown), consistent with the magnetization transfer from natural abundance lipid $^{13}$C to lipid $^1$H. However, there is no systematic intensity buildup for any of the $^1$H peaks on this control sample, confirming that the smooth buildup of the 1,6-colicin data (Fig. 3c, d) contains real distance information.

In theory, the fraction of such lipid background $^1$H intensities is only about twice higher for 1,6-colicin than for pU-colicin due to the two-fold lower $H_{CHH}$ for 1,6-colicin (Table 1). In practice, however, the amount of the lipid-originated $^1$H intensity depends sensitively on the reverse $^{13}$C–$^1$H CP efficiency. The pU-colicin membrane sample contains many rigid backbone protein $^{13}$C sites that transfer the polarization to the $^1$H spins in 150 μs much

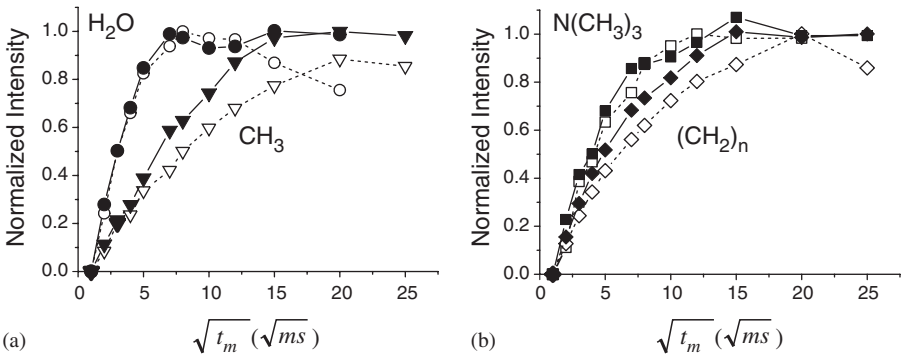


Fig. 6. Effect of the 90° purge pulse on the $^1$H spin diffusion buildup curves obtained from the CHH experiment. pU-colicin was used. The data were collected with the purge pulse on (filled symbols, solid lines) and off (open symbols, dotted lines). The magnetization sources are $H_2O$ (circles), $CH_3$ (triangles), $N(CH_3)_3$ (squares) and $(CH_2)_n$ (diamonds).

more efficiently than the mobile natural-abundance lipid $^{13}C$ sites. Moreover, the optimum Hartman-Hahn match condition for the rigid protein sites can be tailored to differ from the optimum match condition for the mobile lipids. For 1,6-colicin, however, most labeled $^{13}C$ sites occur in the mobile sidechains, whose CP efficiency and match condition are more comparable to the lipid. Thus, it is more difficult to select the protein-originated $^{1}H$ signals against the undesirable lipid-originated $^{1}H$ intensities. Therefore, the CHH experiment is best applied to backbone labeled proteins with high labeling levels. An analogous NHH experiment using a $^{15}N$-labeled protein should also have less natural abundance contribution.

The 1D CHH experiment bears resemblance to the CHHC experiment introduced recently for determining distances within a protein and between proteins [11]. There, the result of $^{1}H$ spin diffusion is detected on $^{13}C$ (or other rare spins) due to the difficulty of direct detection of rigid protons. In our case, this last $^{1}H \rightarrow {}^{13}C$ step is avoided because of the mobility of the lipid and water of interest. Thus, the sensitivity gain from straightforward $^{1}H$ detection, without the need for multiple-pulse decoupling, is an appealing aspect of this CHH technique.

This 1D CHH technique can also be applied to the low-temperature spin diffusion version, where quantitative distance and depth information can be obtained. There, the sensitivity gain will be due to $\gamma$-enhancement only, without the benefit of the reduction of the dimensionality.

## Acknowledgment

The authors thank Prof. K. Schmidt-Rohr for helpful discussions. This work is supported by a CAREER grant from the National Science Foundation (MCB-93387) and a Sloan Research Fellowship to M.H.

## References

[1] K.K. Kumashiro, K. Schmidt-Rohr, O.J. Murphy, K.L. Ouellette, W.A. Cramer, L.K. Thompson, A novel tool for probing membrane protein structure: solid-state NMR with proton spin diffusion and X-nucleus detection, J. Am. Chem. Soc. 120 (1998) 5043.

[2] G.J. Gallagher, M. Hong, L.K. Thompson, Solid-state NMR spin diffusion for measurement of membrane-bound peptide structure: gramicidin A, Biochemistry 43 (2004) 7899.

[3] D. Huster, X.L. Yao, M. Hong, Membrane protein topology probed by 1H spin diffusion from lipids using solid-state NMR spectroscopy, J. Am. Chem. Soc. 124 (2002) 874.

[4] J.J. Buffy, A.J. Waring, R.I. Lehrer, M. Hong, Immobilization and aggregation of antimicrobial peptide protegrin in lipid bilayers investigated by solid-state NMR, Biochemistry 42 (2003) 13725.

[5] D. Huster, X. Yao, K. Jakes, M. Hong, Conformational changes of colicin Ia channel-forming domain upon membrane binding: a solid-state NMR study, Biochim. Biophys. Acta 1561 (2002) 159.

[6] W. Luo, X.L. Yao, M. Hong, Large structure rearrangement of colicin Ia channel domain after membrane binding from 2D 13C spin diffusion NMR, J. Am. Chem. Soc. 127 (2005) 6402.

[7] M. Hong, K. Jakes, Selective and extensive 13C labeling of a membrane protein for solid-state NMR investigation, J. Biomol. NMR 14 (1999) 71.

[8] M. Hong, Determination of multiple phi torsion Angles in solid proteins by selective and extensive 13C labeling and two-dimensional solid-state NMR, J. Magn. Reson. 139 (1999) 389.

[9] A.E. Bennett, C.M. Rienstra, M. Auger, K.V. Lakshmi, R.G. Griffin, Heteronuclear decoupling in rotating solids, J. Chem. Phys. 103 (1995) 6951.

[10] D.J. States, R.A. Haberkorn, D.J. Ruben, A 2D NOE experiment with pure absorption phase in four quadrants, J. Magn. Reson. 48 (1982) 286.

[11] A. Lange, S. Luca, M. Baldus, Structural constraints from proton-mediated rare-spin correlation spectroscopy in rotating solids, J. Am. Chem. Soc. 124 (2002) 9704.